

# Thin-Film Optical Filters



Preparing a plant for the manufacture of narrowband filters. (Courtesy of Walter Nurnberg FIEP FRPS, the editors of *Engineering*, and Sir Howard Grubb, Parsons & Co Ltd.)

# Thin-Film Optical Filters

THIRD EDITION

H A Macleod

*Thin Film Center Inc.  
Tucson, Arizona*

*and*

*Professor Emeritus of Optical Sciences  
University of Arizona*

**IOP**

Institute of Physics Publishing  
Bristol and Philadelphia

© H A Macleod 1986, 2001

All rights reserved. No part of this publication may be reproduced, stored in a retrieval system or transmitted in any form or by any means, electronic, mechanical, photocopying, recording or otherwise, without the prior permission of the publisher. Multiple copying is permitted in accordance with the terms of licences issued by the Copyright Licensing Agency under the terms of its agreement with the Committee of Vice-Chancellors and Principals.

*British Library Cataloguing-in-Publication Data*

A catalogue record for this book is available from the British Library.

ISBN 0 7503 0688 2

*Library of Congress Cataloging-in-Publication Data are available*

Consultant Editor: **Professor W T Welford**, Imperial College, London

Production Editor: Simon Laurenson

Production Control: Sarah Plenty

Cover Design: Victoria Le Billon

Marketing Executive: Colin Fenton

Published by Institute of Physics Publishing, wholly owned by The Institute of Physics, London

Institute of Physics Publishing, Dirac House, Temple Back, Bristol BS1 6BE, UK

US Office: Institute of Physics Publishing, The Public Ledger Building, Suite 1035, 150 South Independence Mall West, Philadelphia, PA 19106, USA

Typeset in T<sub>E</sub>X using the IOP Bookmaker Macros

Printed in the UK by J W Arrowsmith Ltd, Bristol

IPR2025-00845

Apple-Sony EX1028 Page 4

*To*  
*my Mother and Father*  
*Agnes Donaldson Macleod*  
*John Macleod*



# Contents

---

<b>Foreword to the third edition</b>	<b>xiii</b>
<b>Foreword to the second edition</b>	<b>xv</b>
<b>Apologia to the first edition</b>	<b>xix</b>
<b>Symbols and abbreviations</b>	<b>xxiii</b>
<b>1 Introduction</b>	<b>1</b>
1.1 Early history	1
1.2 Thin-film filters	5
References	9
<b>2 Basic theory</b>	<b>12</b>
2.1 Maxwell's equations and plane electromagnetic waves	12
2.1.1 The Poynting vector	17
2.2 The simple boundary	18
2.2.1 Normal incidence	20
2.2.2 Oblique incidence	23
2.2.3 The optical admittance for oblique incidence	27
2.2.4 Normal incidence in absorbing media	29
2.2.5 Oblique incidence in absorbing media	34
2.3 The reflectance of a thin film	37
2.4 The reflectance of an assembly of thin films	40
2.5 Reflectance, transmittance and absorptance	43
2.6 Units	46
2.7 Summary of important results	46
2.8 Potential transmittance	50
2.9 Quarter- and half-wave optical thicknesses	52
2.10 A theorem on the transmittance of a thin-film assembly	53
2.11 Admittance loci	55
2.12 Electric field and losses in the admittance diagram	60
2.13 The vector method	66
2.14 Incoherent reflection at two or more surfaces	67
2.15 Other techniques	72

2.15.1	The Herpin index	72
2.15.2	Alternative method of calculation	73
2.15.3	Smith's method of multilayer design	75
2.15.4	The Smith chart	77
2.15.5	Reflection circle diagrams	80
	References	85
<b>3</b>	<b>Antireflection coatings</b>	<b>86</b>
3.1	Antireflection coatings on high-index substrates	87
3.1.1	The single-layer antireflection coating	87
3.1.2	Double-layer antireflection coatings	92
3.1.3	Multilayer coatings	102
3.2	Antireflection coatings on low-index substrates	108
3.2.1	The single-layer antireflection coating	110
3.2.2	Two-layer antireflection coatings	111
3.2.3	Multilayer antireflection coatings	118
3.3	Equivalent layers	135
3.4	Antireflection coatings for two zeros	139
3.5	Antireflection coatings for the visible and the infrared	144
3.6	Inhomogeneous layers	152
3.7	Further information	156
	References	156
<b>4</b>	<b>Neutral mirrors and beam splitters</b>	<b>158</b>
4.1	High-reflectance mirror coatings	158
4.1.1	Metallic layers	158
4.1.2	Protection of metal films	160
4.1.3	Overall system performance, boosted reflectance	164
4.1.4	Reflecting coatings for the ultraviolet	167
4.2	Neutral beam splitters	169
4.2.1	Beam splitters using metallic layers	169
4.2.2	Beam splitters using dielectric layers	172
4.3	Neutral-density filters	176
	References	177
<b>5</b>	<b>Multilayer high-reflectance coatings</b>	<b>179</b>
5.1	The Fabry–Perot interferometer	179
5.2	Multilayer dielectric coatings	185
5.2.1	All-dielectric multilayers with extended high-reflectance zones	193
5.2.2	Coating uniformity requirements	200
5.3	Losses	204
	References	208

<b>6</b>	<b>Edge filters</b>	<b>210</b>
6.1	Thin-film absorption filters	210
6.2	Interference edge filters	211
6.2.1	The quarter-wave stack	211
6.2.2	Symmetrical multilayers and the Herpin index	213
6.2.3	Performance calculations	223
	References	255
<b>7</b>	<b>Band-pass filters</b>	<b>257</b>
7.1	Broadband-pass filters	257
7.2	Narrowband filters	260
7.2.1	The metal–dielectric Fabry–Perot filter	260
7.2.2	The all-dielectric Fabry–Perot filter	266
7.2.3	The solid etalon filter	280
7.2.4	The effect of varying the angle of incidence	283
7.2.5	Sideband blocking	293
7.3	Multiple cavity filters	293
7.3.1	Thelen’s method of analysis	300
7.4	Higher performance in multiple cavity filters	306
7.4.1	Effect of tilting	315
7.4.2	Losses in multiple cavity filters	316
7.4.3	Case I: high-index cavities	317
7.4.4	Case II: low-index cavities	318
7.4.5	Further information	318
7.5	Phase dispersion filter	319
7.6	Multiple cavity metal–dielectric filters	325
7.6.1	The induced-transmission filter	328
7.6.2	Examples of filter designs	334
7.7	Measured filter performance	342
	References	345
<b>8</b>	<b>Tilted coatings</b>	<b>348</b>
8.1	Introduction	348
8.2	Modified admittances and the tilted admittance diagram	349
8.3	Polarisers	362
8.3.1	The Brewster angle polarising beam splitter	362
8.3.2	Plate polariser	366
8.3.3	Cube polarisers	367
8.4	Nonpolarising coatings	368
8.4.1	Edge filters at intermediate angle of incidence	368
8.4.2	Reflecting coatings at very high angles of incidence	374
8.4.3	Edge filters at very high angles of incidence	376
8.5	Antireflection coatings	377
8.5.1	p-polarisation only	378
8.5.2	s-polarisation only	379

8.5.3	s- and p-polarisation together	381
8.6	Retarders	382
8.6.1	Achromatic quarter- and half-wave retardation plates	382
8.6.2	Multilayer phase retarders	385
8.7	Optical tunnel filters	389
	References	391
<b>9</b>	<b>Production methods and thin-film materials</b>	<b>393</b>
9.1	The production of thin films	394
9.1.1	Thermal evaporation	395
9.1.2	Energetic processes	405
9.1.3	Other processes	413
9.1.4	Baking	417
9.2	Measurement of the optical properties	418
9.3	Measurement of the mechanical properties	436
9.4	Toxicity	445
9.5	Summary of some properties of common materials	446
	References	456
<b>10</b>	<b>Factors affecting layer and coating properties</b>	<b>462</b>
10.1	Microstructure and thin-film behaviour	462
10.2	Sensitivity to contamination	478
	References	485
<b>11</b>	<b>Layer uniformity and thickness monitoring</b>	<b>488</b>
11.1	Uniformity	488
11.1.1	Flat plate	490
11.1.2	Spherical surface	490
11.1.3	Rotating substrates	490
11.2	Substrate preparation	497
11.3	Thickness monitoring	499
11.3.1	Optical monitoring techniques	500
11.3.2	The quartz-crystal monitor	509
11.4	Tolerances	511
	References	520
<b>12</b>	<b>Specification of filters and environmental effects</b>	<b>523</b>
12.1	Optical properties	523
12.1.1	Performance specification	523
12.1.2	Manufacturing Specification	526
12.1.3	Test Specification	527
12.2	Physical properties	530
12.2.1	Abrasion Resistance	530
12.2.2	Adhesion	533
12.2.3	Environmental Resistance	533
	References	535

<b>13 System considerations: applications of filters and coatings</b>	<b>536</b>
13.1 Potential energy grasp of interference filters	540
13.2 Narrowband filters in astronomy	545
13.3 Atmospheric temperature sounding	550
13.4 Order-sorting filters for grating spectrometers	559
13.5 Glare suppression filters and coatings	570
13.6 Some coatings involving metal layers	575
13.6.1 Electrode films for Schottky-barrier photodiodes	575
13.6.2 Spectrally selective coatings for photothermal solar energy conversion	579
13.6.3 Heat reflecting metal–dielectric coatings	583
References	585
<b>14 Other topics</b>	<b>588</b>
14.1 Rugate filters	588
14.2 Ultrafast coatings	599
14.3 Automatic methods	610
References	619
<b>15 Characteristics of thin-film dielectric materials</b>	<b>621</b>
References	628
<b>Index</b>	<b>631</b>

# Chapter 3

---

## Antireflection coatings

As has already been mentioned in chapter 1, antireflection coatings were the principal objective of much of the early work in thin-film optics. Of all the possible applications, antireflection coatings have had the greatest impact on technical optics, and even today, in sheer volume of production, they still exceed all other types of coating. In some applications, antireflection coatings are simply required for the reduction of surface reflection. In others, not only must surface reflection be reduced, but the transmittance must also be increased. The crown glass elements in a compound lens have a transmittance of only 96% per untreated surface, while the flint components can have a surface transmittance as low as 90%. The net transmittance of even a modest number of untreated elements in series can therefore be quite low. Additionally, part of the light reflected at the various surfaces eventually reaches the focal plane, where it appears as ghosts or as a veiling glare, thus reducing the contrast of the images. This is especially true of the zoom lenses used in television or photography, where 20 or more elements may be included, and which would be completely unusable without antireflection coatings.

Antireflection coatings can range from a simple single layer having virtually zero reflectance at just one wavelength, to a multilayer system of more than a dozen layers, having virtually zero reflectance over a range of several octaves. The type used in any particular application will depend on a variety of factors, including the substrate material, the wavelength region, the required performance and the cost.

In the visible region, crown glass, which has a refractive index of around 1.52, is most commonly used. As we shall see, this presents a very different problem from infrared materials, which can have very much higher refractive indices. It is convenient, therefore, to split what follows into antireflection coatings for low-index substrates and antireflection coatings for high-index substrates, corresponding roughly to the visible and infrared. Since, from the point of view of design, antireflection coatings for high-index substrates are more straightforward, they are considered first.

There is no systematic method for the design of antireflection coatings. Trial and error, assisted by approximate techniques (frequently one or other of the graphical methods mentioned in chapter 2) backed up by accurate computer calculation, are frequently employed. Very promising designs can be further improved by computer refinement. Several different approaches are used in this chapter, partly to illustrate their use and partly because they are complementary. All the performance curves have been computed by application of the matrix method. In most cases, the materials are considered to be completely transparent.

The vast majority of antireflection coatings are required for matching an optical element into air. Air has an index of around 1.0003 at standard temperature and pressure which, for practical purposes, can be considered as unity. The earliest antireflection coatings were on glass for use in the visible region of the spectrum. As shall become apparent later, a single-layer antireflection coating on glass, for the centre of the visible region, has a distinct magenta tinge when examined visually in reflection. This gives an appearance not unlike tarnish, and indeed in chapter 1 we mentioned the beneficial effects of the tarnish layer on aged flint objectives, and so the term 'bloom', in the sense of tarnish, has been used in this connection. The action of applying the coating is referred to as 'blooming' and the element is said to be 'bloomed'.

### **3.1 Antireflection coatings on high-index substrates**

The term high index in this context cannot be defined precisely in the sense of a range with a definite lower bound. It simply means that the substrate has an index sufficiently higher than the available thin-film materials to enable the design of high-performance antireflection coatings consisting entirely, or almost entirely, of layers with indices lower than that of the substrate. These high-index substrates are principally of use in the infrared. Semiconductors, such as germanium, with an index of around 4.0, giving a reflection loss of around 36% per surface, and silicon, with an index around 3.5 and reflection loss of 31%, are common, and it would be completely impossible to use them in the vast majority of applications without some form of antireflection coating. For many purposes, the reduction of a 30% reflection loss to one of a few per cent would be considered adequate. It is only in a limited number of applications where the reflection loss must be reduced to less than 1%.

#### **3.1.1 The single-layer antireflection coating**

The simplest form of antireflection coating is a single layer. Consider figure 3.1. Here we have a vector diagram which, since two interfaces are involved, contains two vectors, each representing the amplitude reflection coefficient at an interface.

If the incident medium is air, then, provided the index of the film is lower than the index of the substrate, the reflection coefficient at each interface will be negative, denoting a phase change of  $180^\circ$ . The resultant locus is a circle with a

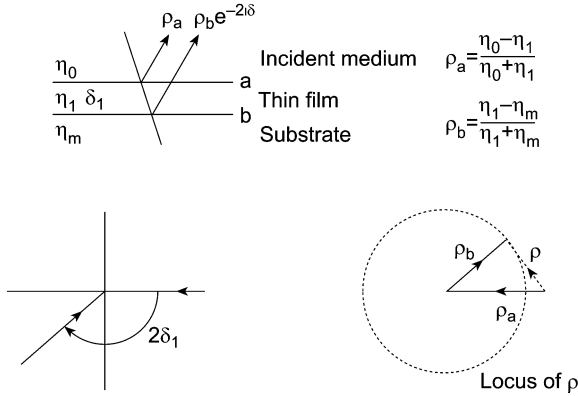


Figure 3.1. Vector diagram of a single-layer antireflection coating.

minimum at the wavelength for which the phase thickness of the layer is  $90^\circ$ , that is, a quarter-wave optical thickness, when the two vectors are completely opposed. Complete cancellation at this wavelength, that is, zero reflectance, will occur if the vectors are of equal length. This condition, in the notation of figure 3.1, is

$$\frac{y_0 - y_1}{y_0 + y_1} = \frac{y_1 - y_m}{y_1 + y_m}$$

which requires

$$\frac{y_1}{y_0} = \frac{y_m}{y_1}$$

or

$$y_1 = (y_0 y_m)^{1/2}, \tag{3.1}$$

which at optical frequencies can also be written

$$n_1 = (n_0 n_m)^{1/2}.$$

At oblique incidence, the admittances,  $y$ , in (3.1) should be replaced by the appropriate tilted values,  $\eta$ .

Although this result was derived by an approximate technique, the result is exactly correct. We recall that in chapter 2 it was shown that the optical admittance of a substrate coated with a quarter-wave optical thickness is

$$Y = y_1^2 / y_m,$$

where  $y_1$  is the admittance of the film material and  $y_m$  that of the substrate. The reflectance is therefore given by

$$R = \left( \frac{y_0 - Y}{y_0 + Y} \right)^2 = \left( \frac{y_0 - y_1^2 / y_m}{y_0 + y_1^2 / y_m} \right)^2.$$

This is an exact result and clearly the reflectance is zero if  $y_1$  is given by (3.1).

The condition for a perfect single-layer antireflection coating is, therefore, a quarter-wave optical thickness of material with optical admittance equal to the square root of the product of the admittances of substrate and medium. It is seldom possible to find a material of exactly the optical admittance which is required. If there is a small error,  $\varepsilon$ , in  $y_1$  such that

$$y_1 = (1 + \varepsilon)(y_0 y_m)^{1/2}$$

then

$$R = \left( \frac{-2\varepsilon - \varepsilon^2}{2 + 2\varepsilon + \varepsilon^2} \right)^2 \approx \varepsilon^2$$

provided that  $\varepsilon$  is small. A 10% error in  $y_1$ , therefore, leads to a residual reflectance of 1%.

Zinc sulphide has an index of around 2.2 at  $2 \mu\text{m}$  and 2.15 at  $15 \mu\text{m}$ . It has sufficient transparency for use as a quarter-wave antireflection coating over the range  $0.4\text{--}25 \mu\text{m}$ . Germanium, silicon, gallium arsenide, indium arsenide and indium antimonide can all be treated satisfactorily by a single layer of zinc sulphide. The procedure to be followed for hard, rugged zinc sulphide films is described in a paper by Cox and Hass [1]. The substrate should be maintained at around  $150^\circ\text{C}$  during coating and cleaned by a glow discharge immediately before coating. The transmittance of a germanium plate with a single-layer zinc sulphide antireflection coating is shown in figure 3.2.

Zinc sulphide, even deposited under the best conditions, can deteriorate after prolonged exposure to humid atmospheres. Somewhat harder and more robust coatings are produced with cerium oxide or silicon monoxide. Cerium oxide, when deposited at a substrate temperature of  $200^\circ\text{C}$  or more, forms very hard and durable films of refractive index 2.2 at  $2 \mu\text{m}$ . Unfortunately, in common with many other materials it displays a slight absorption band at  $3 \mu\text{m}$  owing to adsorbed water vapour. Silicon monoxide does not show this water vapour band to the same degree, and so Cox and Hass have recommended this material as the most satisfactory for coating germanium and silicon in the near infrared. The index of silicon monoxide evaporated in a good vacuum at a high rate is around 1.9. The transmittance of a silicon plate coated on both sides with silicon monoxide is shown in figure 3.3.

So far, we have considered only normal incidence in the numerical calculations which we have made. At angles of incidence other than normal, the behaviour is similar, but the effective phase thickness of the layer is reduced as the incidence increases due to the cosine term in the phase thickness

$$\delta = (2\pi nd \cos \vartheta) / \lambda$$

and so the optimum wavelength is shorter. For the optical admittance we must use the appropriate  $\eta_p$  or  $\eta_s$ , and, as these are different, polarisation effects become

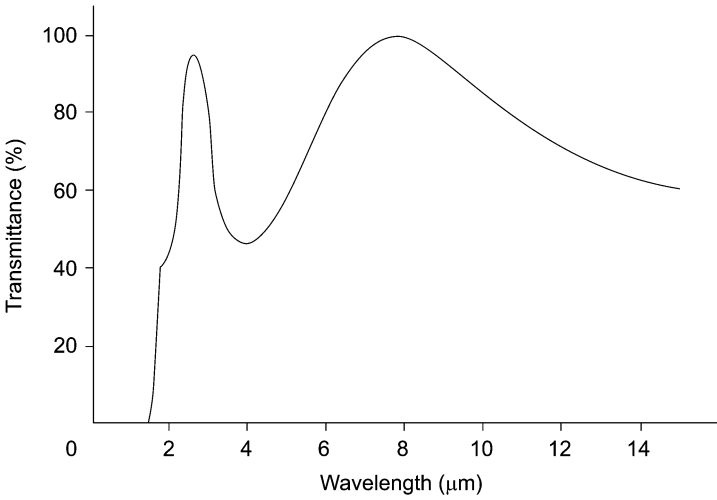


**Figure 3.2.** Transmittance of a germanium plate bloomed on both sides with zinc sulphide for 8 μm. (Courtesy of Sir Howard Grubb, Parsons & Co. Ltd.)

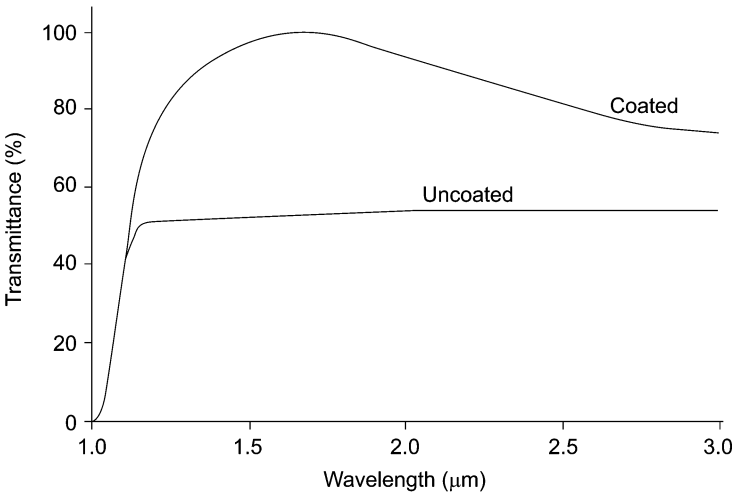


**Figure 3.3.** Transmittance of a 1.5-mm thick silicon plate with and without antireflection coatings of silicon monoxide, a quarter-wavelength thick at 1.7 μm. (After Cox and Hass [1].)

evident. For high-index substrates and coatings the effects are much less than for the low-index coatings for the visible region, as we shall see later. Figure 3.4 shows the calculated variation with angle of incidence of the performance of a

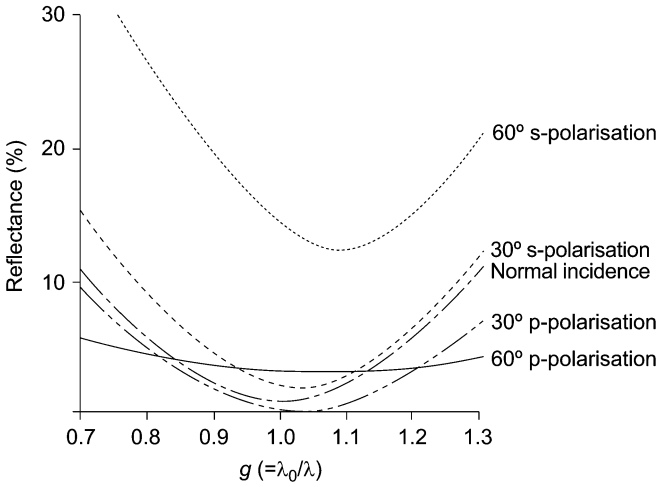


**Figure 3.4.** Calculated performance at various angles of incidence of a zinc sulphide coating ( $n = 2.2$ ) on a germanium substrate ( $n = 4.0$ ).

zinc sulphide coating ( $n = 2.2$ ) on a germanium substrate ( $n = 4.0$ ).

Such calculations are relatively straightforward. If we use the matrix method, the characteristic matrix of a single film on a substrate is given by

$$\begin{bmatrix} B \\ C \end{bmatrix} = \begin{bmatrix} \cos \delta_1 & \frac{i \sin \delta_1}{\eta_1} \\ i \eta_1 \sin \delta_1 & \cos \delta_1 \end{bmatrix} \begin{bmatrix} 1 \\ \eta_m \end{bmatrix},$$

i.e.

$$\begin{bmatrix} B \\ C \end{bmatrix} = \begin{bmatrix} \cos \delta_1 + i (\eta_m / \eta_1) \sin \delta_1 \\ \eta_m \cos \delta_1 + i \eta_1 \sin \delta_1 \end{bmatrix},$$

where the symbols have the meanings, defined in chapter 2,

$$\left. \begin{aligned} \eta_p &= y / \cos \vartheta \\ \eta_s &= y \cos \vartheta \end{aligned} \right\} \text{for each material}$$

$$\delta_1 = (2\pi n_1 d_1 \cos \vartheta_1) / \lambda$$

and where

$$n_0 \sin \vartheta_0 = n_1 \sin \vartheta_1 = n_m \sin \vartheta_m.$$

If  $\lambda_0$  is the wavelength for which the layer is a quarter-wave optical thickness at normal incidence, then  $n_1 d_1 = \lambda_0 / 4$  and

$$\delta_1 = \frac{\pi}{2} \left( \frac{\lambda_0}{\lambda} \right) \cos \vartheta_1$$

so that the new optimum wavelength is  $\lambda_0 \cos \vartheta_1$ .

The amplitude reflection coefficient is

$$\begin{aligned} \rho &= \frac{\eta_0 - Y}{\eta_0 + Y} = \frac{\eta_0 - C/B}{\eta_0 + C/B} \\ &= \frac{(\eta_0 - \eta_m) \cos \delta_1 + i[(\eta_0 \eta_m / \eta_1) - \eta_1] \sin \delta_1}{(\eta_0 + \eta_m) \cos \delta_1 + i[(\eta_0 \eta_m / \eta_1) + \eta_1] \sin \delta_1} \end{aligned} \quad (3.2)$$

and the reflectance

$$R = \frac{(\eta_0 - \eta_m)^2 \cos^2 \delta_1 + i[(\eta_0 \eta_m / \eta_1) - \eta_1]^2 \sin^2 \delta_1}{(\eta_0 + \eta_m)^2 \cos^2 \delta_1 + i[(\eta_0 \eta_m / \eta_1) + \eta_1]^2 \sin^2 \delta_1}. \quad (3.3)$$

This expression is deceptively simple. An increase in the number of layers or a move to an absorbing system immediately increases the complexity to a degree that is completely discouraging.

It is instructive to prepare an admittance diagram (figure 3.5) for the single-layer coating. We recall that admittance loci were discussed in chapter 2. We consider normal incidence only and use free space units for the admittances so that they are numerically equal to the refractive indices. The locus for a single layer is a circle and in this case it begins at the point 4.0 on the real axis, corresponding to the admittance of the germanium substrate. The centre of the circle is on the real axis and the circle cuts the real axis again at the point  $2.2^2/4.0 = 1.21$ , corresponding to a quarter-wave optical thickness. Note especially that since the two points of intersection with the real axis are defined we do not need to calculate the position of the centre. We can mark a scale of  $\delta_1$  along the locus. Since  $\delta_1 = 2\pi n_1 d_1 / \lambda$ , we can either assume  $\lambda$  constant and replace the scale with one of optical thickness, or, provided that we assume that the refractive index remains constant with wavelength, for a given layer optical thickness we can mark the scale in terms of  $g$  ( $= \lambda_0 / \lambda$ ). These various scales have been added. The scale of  $g$  assumes that  $\lambda_0$  is the wavelength for which the layer has an optical thickness of one quarter-wave.

This is a particularly simple admittance locus and it is included principally to illustrate the method. We will make some use of admittance diagrams in this chapter. Normally these will be drawn for one value of wavelength and for one value of optical thickness for each layer.

### 3.1.2 Double-layer antireflection coatings

The disadvantage of the single-layer coating, as far as the design is concerned, is the limited number of adjustable parameters. We can see from the admittance locus of figure 3.5 that only where the locus passes through the point (1, 0) will zero reflectance be obtained (or more generally when the locus passes through the point  $(y_0, 0)$ ) and this must correspond to a semicircle or a quarter-wave optical thickness (or, strictly, an odd integral multiple thereof). The refractive index, or

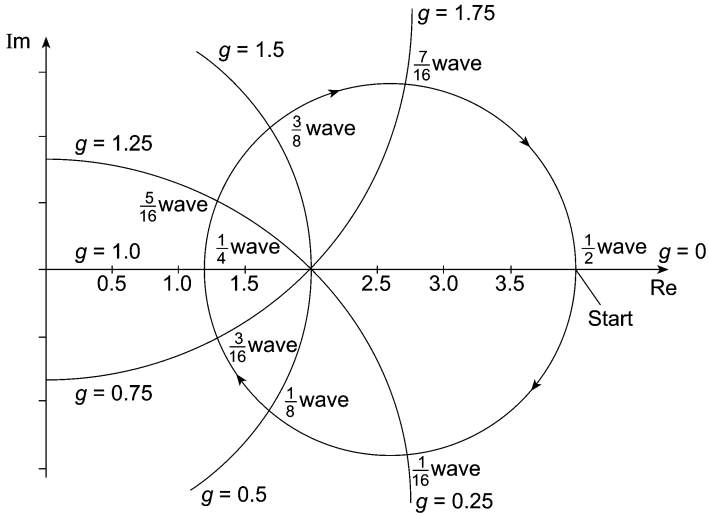


**Figure 3.5.** Admittance diagram for a single-layer zinc sulphide ( $n = 2.2$ ) coating on germanium ( $n = 4.0$ ).

optical admittance, of the layer is also uniquely determined as  $y_1 = (y_0 y_m)^{1/2}$ . There is thus no room for manoeuvre in the design of a single-layer coating. In practice, the refractive index is not a parameter that can be varied at will. Materials suitable for use as thin films are limited in number and the designer has to use what is available. A more rewarding approach, therefore, is to use more layers, specifying obtainable refractive indices for all layers at the start, and to achieve zero reflectance by varying the thickness. Then, too, there is the limitation that the single-layer coating can give zero reflectance at one wavelength only and low reflectance over a narrow region. A wider region of high performance demands additional layers.

Much of this design work nowadays is carried out by automatic methods and this is a perfectly sensible and efficient development. Automatic methods are briefly described elsewhere in this book. They are particularly valuable for antireflection coatings and are strongly recommended. Here, however, we are concerned also with the understanding of the structures of the coatings and particularly with the parts played by the individual layers. Without such understanding we are completely vulnerable when things go wrong and the results are not as expected. Also, automatic design techniques function more efficiently when they are furnished with good starting designs. We therefore spend much time in this chapter with some of the traditional design techniques, not so much because all are still used in actual design work, but because they require a knowledge of the structure and working of the coatings, and because they are interesting.

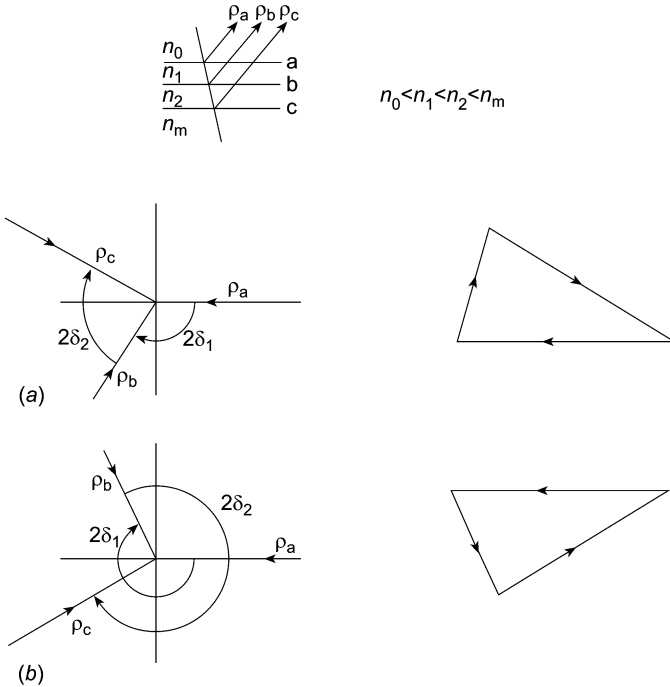


**Figure 3.6.** Vector diagram for a double-layer antireflection coating. The thickness of the layers can be chosen to close the vector triangle and give zero reflectance in two ways, (a) and (b).

We will consider first the problem of ensuring zero reflectance at one single wavelength and we shall attempt to achieve this with a two-layer coating. Since we are dealing with high-index substrates we look initially at combinations of layers having refractive indices lower than that of the substrate. A vector diagram of one possibility is shown in figure 3.6. Provided the vectors are not such that any one is greater in length than the sum of the other two, then there are two sets of thicknesses for which zero reflectance can be obtained at one wavelength. The thinner combination, as in figure 3.6(a), will give the broadest characteristic and should normally be chosen. In some ways, it is easier to visualise the design using an admittance plot. As usual, we plot admittance in free space units so that it is numerically the same as the refractive index. Two possible arrangements are shown in figure 3.7, which can be obtained simply by drawing the circle corresponding to index  $n_1$ , passing through the point  $n_0$ , and the circle corresponding to index  $n_2$  passing through the point  $n_m$ . Provided these circles intersect, then it is possible to use them as an antireflection coating. The two sets of thicknesses correspond to the two points of intersection.

This is a very important coating with wider implications than just the

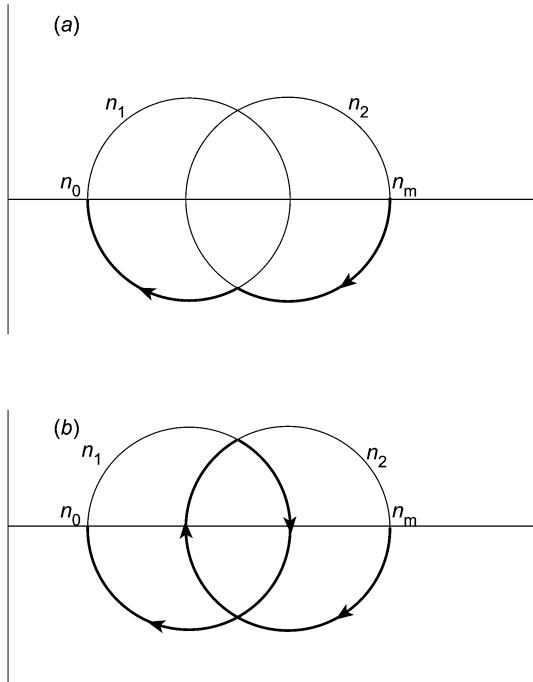


**Figure 3.7.** Admittance diagram for the double-layer antireflection coating. The two possible solutions are shown in (a) and (b).

blooming of a high-index substrate and so it is worth examining in greater detail. We use the matrix method and follow an analysis by Catalan [2], changing the notation to agree with the system used here. The characteristic matrix of the assembly is

$$\begin{aligned} \begin{bmatrix} B \\ C \end{bmatrix} &= \begin{bmatrix} \cos \delta_1 & \frac{i \sin \delta_1}{y_1} \\ iy_1 \sin \delta_1 & \cos \delta_1 \end{bmatrix} \begin{bmatrix} \cos \delta_2 & \frac{i \sin \delta_2}{y_2} \\ iy_2 \sin \delta_2 & \cos \delta_2 \end{bmatrix} \begin{bmatrix} 1 \\ y_m \end{bmatrix} \\ &= \begin{bmatrix} \cos \delta_1 [\cos \delta_2 + i (y_m/y_2) \sin \delta_2] + i \sin \delta_1 (y_m \cos \delta_2 + iy_2 \sin \delta_2) / y_1 \\ iy_1 \sin \delta_1 [\cos \delta_2 + i (y_m/y_2) \sin \delta_2] + \cos \delta_1 (y_m \cos \delta_2 + iy_2 \sin \delta_2) \end{bmatrix}. \end{aligned}$$

The reflectance will be zero if the optical admittance  $Y$  is equal to  $y_0$ , i.e.

$$\begin{aligned} iy_1 \sin \delta_1 [\cos \delta_2 + i (y_m/y_2) \sin \delta_2] + \cos \delta_1 (y_m \cos \delta_2 + iy_2 \sin \delta_2) \\ = y_0 \{ \cos \delta_1 [\cos \delta_2 + i (y_m/y_2) \sin \delta_2] + i \sin \delta_1 (y_m \cos \delta_2 + iy_2 \sin \delta_2) / y_1 \}. \end{aligned}$$

The real and imaginary parts of these expressions must be equated separately giving

$$\begin{aligned} - (y_1 y_m / y_2) \sin \delta_1 \sin \delta_2 + y_m \cos \delta_1 \cos \delta_2 \\ = y_0 \cos \delta_1 \cos \delta_2 - (y_0 y_2 / y_1) \sin \delta_1 \sin \delta_2 \end{aligned}$$

and

$$\begin{aligned} y_1 \sin \delta_1 \cos \delta_2 + y_2 \cos \delta_1 \sin \delta_2 \\ = (y_0 y_m / y_2) \cos \delta_1 \sin \delta_2 + (y_0 y_m / y_1) \sin \delta_1 \cos \delta_2 \end{aligned}$$

i.e.

$$\begin{aligned} \tan \delta_1 \tan \delta_2 &= (y_m - y_0)[(y_1 y_m / y_2) - (y_0 y_2 / y_1)] \\ &= y_1 y_2 (y_m - y_0)(y_1^2 y_m - y_0 y_2^2) \end{aligned} \quad (3.4)$$

and

$$\tan \delta_2 / \tan \delta_1 = y_2 (y_0 y_m - y_1^2) / [y_1 (y_2^2 - y_0 y_m)] \quad (3.5)$$

giving

$$\begin{aligned} \tan^2 \delta_1 &= \frac{(y_m - y_0)(y_2^2 - y_0 y_m)y_1^2}{(y_1^2 y_m - y_0 y_2^2)(y_0 y_m - y_1^2)} \\ \tan^2 \delta_2 &= \frac{(y_m - y_0)(y_0 y_m - y_1^2)y_2^2}{(y_1^2 y_m - y_0 y_2^2)(y_2^2 - y_0 y_m)}. \end{aligned} \quad (3.6)$$

The values of  $\delta_1$  and  $\delta_2$  found from these equations must be correctly paired and this is most easily done either by ensuring that they also satisfy the two preceding equations or by sketching a rough admittance diagram.

For solutions to exist, or, putting it in another way, for the circles in the admittance diagram to intersect, the right-hand sides of equations (3.6) must be positive.  $\delta_1$  and  $\delta_2$  are then real. This requires that, of the expressions

$$(y_2^2 - y_0 y_m) \quad (3.7)$$

$$(y_1^2 y_m - y_0 y_2^2) \quad (3.8)$$

$$(y_0 y_m - y_1^2) \quad (3.9)$$

either all three must be positive or any two are negative and the third positive. This can be summarised in a useful diagram (figure 3.8) known as a Schuster diagram after one of the originators [3]. The bottom right-hand part of the diagram corresponds to the validity conditions given in figure 3.7.

One useful coating is given by the area at the top left-hand edge of the diagram where  $y_1 \geq (y_0 y_m)^{1/2} \geq y_2$ . For germanium at normal incidence in air,  $(y_0 y_m)^{1/2} = 2.0$ . There is no upper limit to the magnitude of  $y_1$ , which can be conveniently chosen to be germanium with index 4.0, while  $y_2$  can be magnesium fluoride with index 1.38, didymium fluoride with index 1.57, cerium fluoride with index 1.59, or any other similar material. The advantage of this arrangement is that the low-index film, which tends to be less robust, is protected by the high-index layer. Germanium layers are particularly good in this respect. Figure 3.9 gives an example of this type of coating. Generally, the total thickness, as in the example, is rather thinner than a quarter-wave, which adds to the durability. Cox [4] has discussed a number of different possibilities along these lines.

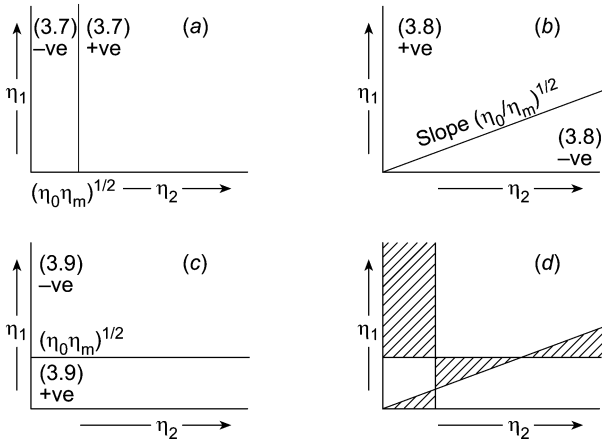


**Figure 3.8.** The construction of a Schuster diagram. (a), (b) and (c) are combined in one diagram in (d) and the shaded areas are those in which real solutions exist.

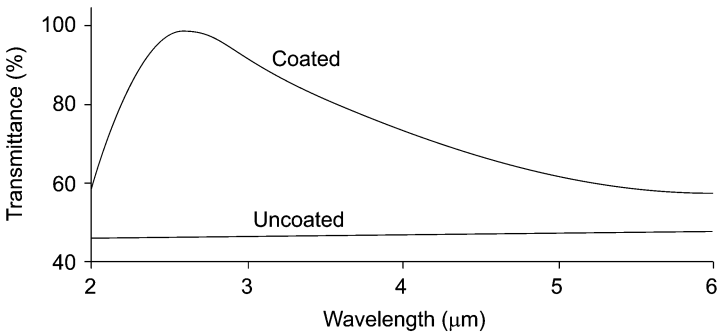


**Figure 3.9.** Transmittance of a germanium plate with two-layer antireflection coatings of MgF<sub>2</sub>, ( $nd = \lambda/4$  at 1.03  $\mu\text{m}$ ) and germanium ( $nd = \lambda/4$  at 0.61  $\mu\text{m}$ ), the germanium being the outermost layer. (After Cox [4].)

Unfortunately, this type of double-layer coating tends to have rather narrower useful ranges than the single-layer coating, which may itself not be broad enough for certain applications. It is possible to broaden the region of reflectance by using two, or even more, layers. A common approach is to choose layer thicknesses which are whole numbers of quarter-waves, and then to determine the refractive indices which should be used to give the desired performance.

An effective coating is one consisting of two quarter-wave layers (see figure 3.10). The appearances of the vector diagram at three different wavelengths is shown in (a), (b) and (c). At  $\lambda = (3/4)\lambda_0$  and  $\lambda = (3/2)\lambda_0$  the three vectors in the triangle are inclined at  $60^\circ$  to each other. Provided the vectors are all of

equal length, the triangles will be closed and the reflectance will be zero at these wavelengths. This condition can be written

$$\frac{y_1}{y_0} = \frac{y_2}{y_1} = \frac{y_m}{y_2}$$

and solved for  $y_1$  and  $y_2$ :

$$\begin{aligned} y_1^3 &= y_0^2 y_m \\ y_2^3 &= y_0 y_m^2. \end{aligned} \tag{3.10}$$

The reflectance at the reference wavelength  $\lambda_0$  where the layers are quarter-waves is given by

$$\begin{aligned} R &= \left( \frac{y_0 - (y_1^2/y_2^2) y_m}{y_0 + (y_1^2/y_2^2) y_m} \right)^2 \\ &= \left( \frac{1 - (y_m/y_0)^{1/3}}{1 + (y_m/y_0)^{1/3}} \right)^2, \end{aligned}$$

a considerable improvement over the bare substrate.

For germanium of refractive index 4.0 in air, at normal incidence, the values required for the indices are  $n_1 = 1.59$  and  $n_2 = 2.50$  and the reflectance at  $\lambda_0$  is 5.6%. The theoretical curve of this coating is shown in figure 3.11(a). Theoretical and measured curves of a similar coating on arsenic trisulphide and triselenide are given in figure 3.11(b) and (c).

The coating just described is a special case of a general coating where the layers are of equal thickness. To compute the general conditions it is easiest to return to the analysis leading up to equations (3.6).

Let  $\delta_1$  be set equal to  $\delta_2$  and denoted by  $\delta$ , where we recall that if  $\lambda_0$  is the wavelength for which the layers are quarter-waves then

$$\delta = \frac{\pi}{2} \left( \frac{\lambda_0}{\lambda} \right).$$

From equation (3.5)

$$y_2(y_0 y_m - y_1^2) = y_1(y_2^2 - y_0 y_m),$$

i.e.

$$y_0 y_m = y_1 y_2$$

which is a necessary condition for zero reflectance.

From equation (3.4) we find the wavelengths  $\lambda$  corresponding to zero reflectance

$$\tan^2 \delta = \frac{y_1 y_2 (y_m - y_0)}{y_1^2 y_m - y_0 y_2^2} = \frac{y_0 y_m (y_m - y_0)}{y_1^2 y_m - y_0 y_2^2}.$$

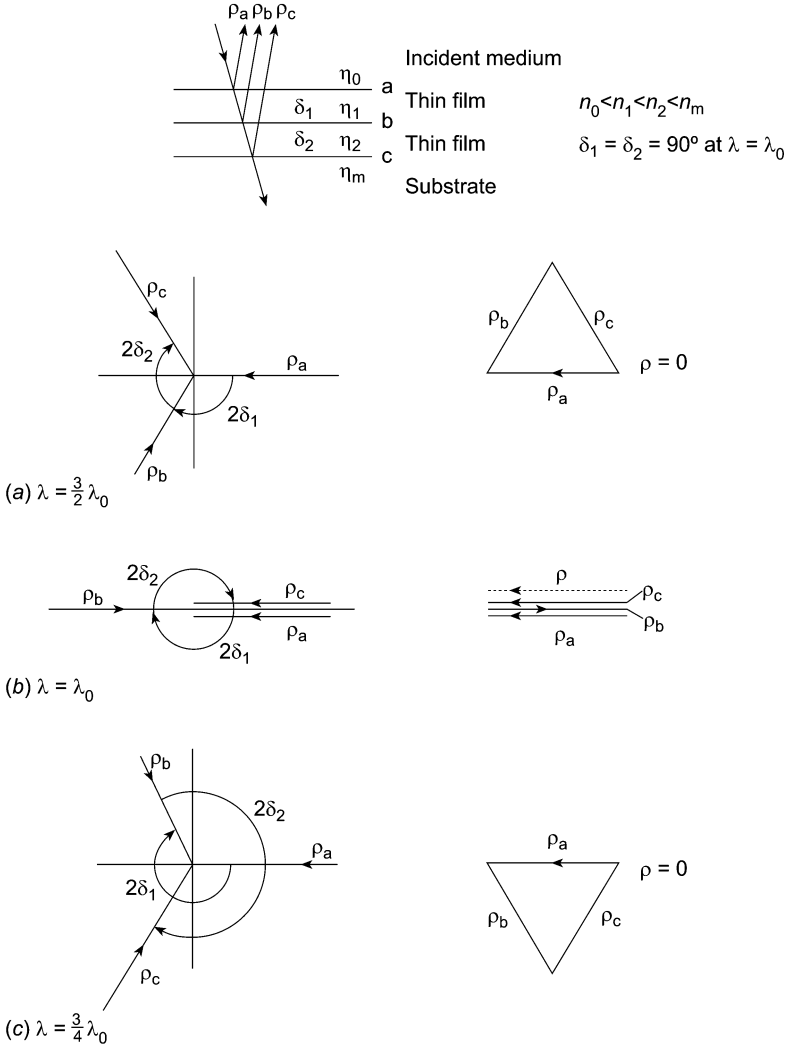


**Figure 3.10.** Vector diagrams for quarter-quarter antireflection coatings on a high-index substrate.

If  $\delta$  is the solution in the first quadrant then there are two solutions

$$\delta = \delta' \quad \text{or} \quad \delta = \pi - \delta'$$

and the two values of  $\lambda$  are

$$\lambda = \left( \frac{\pi/2}{\delta} \right) \lambda_0.$$

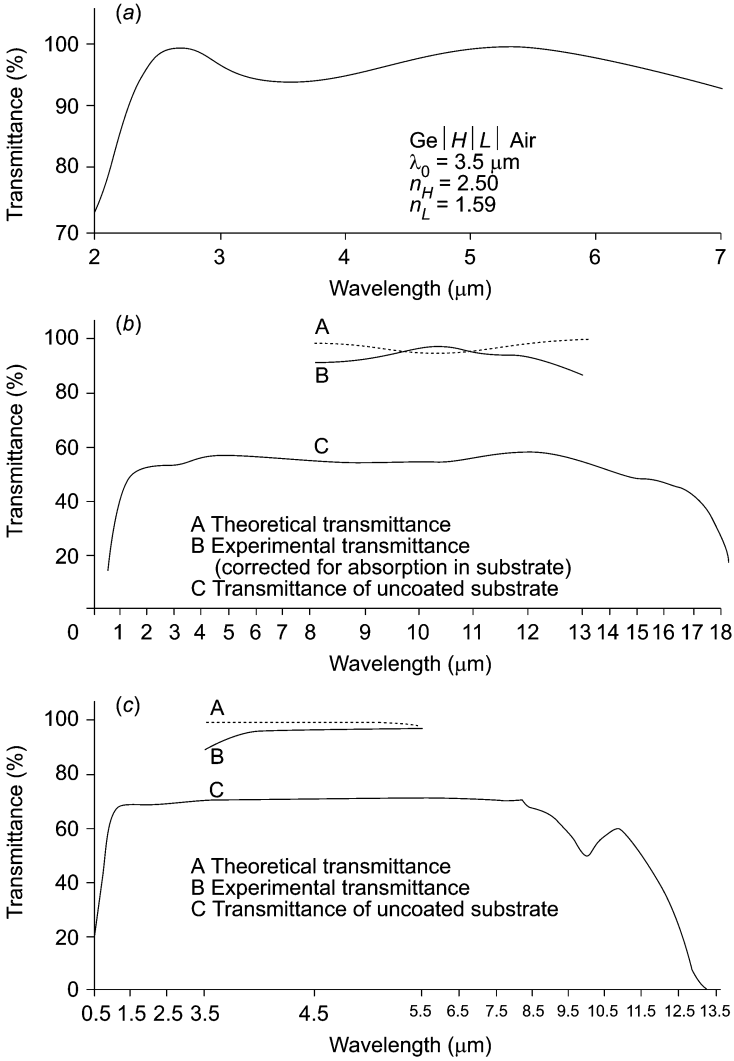


**Figure 3.11.** Double-layer antireflection coatings for high-index substrates. (a) Theoretical transmittance of a quarter-quarter coating on germanium (single surface). (b) Theoretical and measured transmittance of a similar coating on arsenic trisulphide glass (double surface). (c) Theoretical and measured transmittance of a similar coating on arsenic triselenide glass (double surface). ((b) and (c) by courtesy of Barr and Stroud Ltd.)

In all practical cases,  $y_m$  will be greater than  $y_0$  and the above equation for  $\tan^2 \delta$  will have a real solution provided

$$y_1^2 y_m - y_0 y_2^2 \geq 0.$$

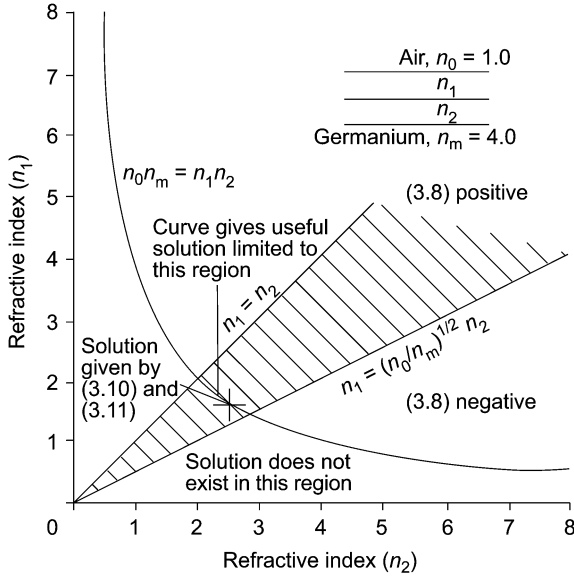


**Figure 3.12.** A Schuster diagram showing possible values of film indices for a quarter-quarter coating on germanium.

The left-hand side of this inequality is identical to expression (3.8).

Figure 3.12 gives the allowed values of  $y_1$  and  $y_2$  for germanium in air plotted on a Schuster diagram assuming normal incidence. The form of the characteristic curve of the coating is similar to that of figure 3.11. The reflectance rises to a maximum value at the reference wavelength  $\lambda_0$  situated between the two zeros. The reflectance at  $\lambda_0$  can be found quite simply. At this wavelength,  $\delta = \pi/2$  and the layers are quarter-waves. The optical admittance is given, therefore, by

$$\frac{y_1^2}{y_2^2} y_m$$

and the reflectance by

$$R = \left( \frac{y_0 - (y_1^2/y_2^2) y_m}{y_0 + (y_1^2/y_2^2) y_m} \right)^2 \tag{3.11}$$

We are considering cases where  $y_m$  is large. For  $y_1 = y_2$ , the reflectance at  $\lambda_0$  is that of the bare substrate. If  $y_1 > y_2$  the reflectance is even higher. Thus, for the solution to be at all useful,  $y_1$  should be less than  $y_2$  and the region where this condition holds is indicated on the diagram.

### 3.1.3 Multilayer coatings

Figure 3.13 shows a vector diagram for a three-layer coating on germanium. Each layer is a quarter-wave thick at  $\lambda_0$ . If  $y_m > y_3 > y_2 > y_1 > y_0$  then the vectors will oppose each other, as shown, at  $(2/3)\lambda_0$ ,  $\lambda_0$  and  $2\lambda_0$ , and, provided the vectors are all of equal length, will completely cancel at these wavelengths, giving zero reflectance.

This coating is similar to the quarter-quarter coating of figure 3.10, but where the two zeros of the two-layer coating are situated at  $(3/4)\lambda_0$  and  $(3/2)\lambda_0$ , those of this three-layer coating stretch from  $(2/3)\lambda_0$  to  $2\lambda_0$ , a much broader region.

The condition for the vectors to be of equal length is

$$\frac{y_1}{y_0} = \frac{y_2}{y_1} = \frac{y_3}{y_2} = \frac{y_m}{y_3}$$

which with some manipulation becomes

$$\begin{aligned} y_1^4 &= y_0^3 y_m \\ y_2^4 &= y_0^2 y_m^2 \\ y_3^4 &= y_0 y_m^3 \end{aligned} \quad (3.12)$$

For germanium in air at normal incidence

$$n_0 = 1.00 \quad n_m = 4.00$$

and the refractive indices required for the layers are

$$\begin{aligned} n_1 &= 1.41 \\ n_2 &= 2.00 \\ n_3 &= 2.83. \end{aligned}$$

A coating which is not far removed from these theoretical figures is silicon, next to the substrate, of index 3.3, followed by cerium oxide of index 2.2, followed by magnesium fluoride, index 1.35. The performance of such a coating with  $\lambda_0 = 3.5 \mu\text{m}$  is shown in figure 3.14. This coating, along with other one- and two-layer coatings for the infrared, is described by Cox *et al* [5]. The exact theory of this coating may be developed in the same way as that of the two-layer coating, but the calculations are more involved.

It is relatively easy to extend the vector method to deal with four layers, where the zeros of reflectance are found at  $(5/8)\lambda_0$ ,  $(5/6)\lambda_0$ ,  $(5/4)\lambda_0$  and  $(5/2)\lambda_0$ , an even broader region than the three-layer coating. Five layers are equally straightforward. Whether or not such coatings are of practical value depends very much on the application. For many purposes the two-layer coating is quite adequate.

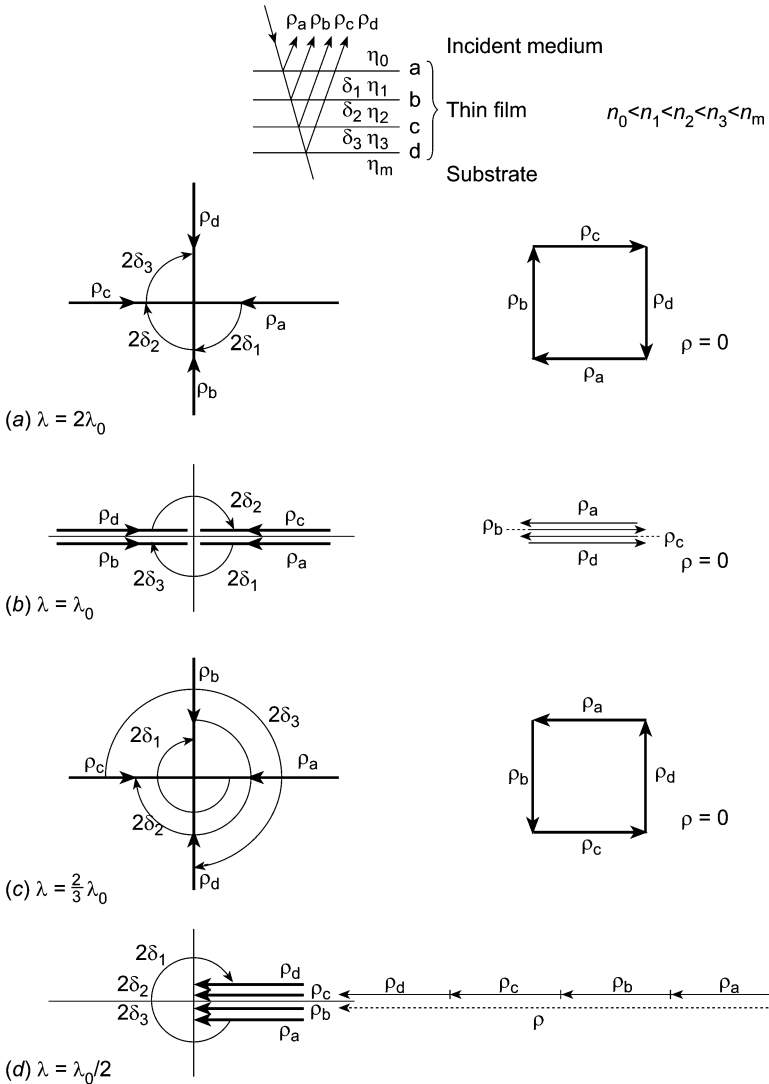


**Figure 3.13.** Vector diagram for a quarter-quarter-quarter coating on a high-index substrate.

The addition of an extra layer makes the exact theory of the three-layer coating very much more involved than that of the two-layer. The number of possible groups of designs is enormous. It therefore becomes profitable to employ techniques which, rather than calculate performance in detail, simply indicate arrangements which are likely to be capable of acceptable performance and

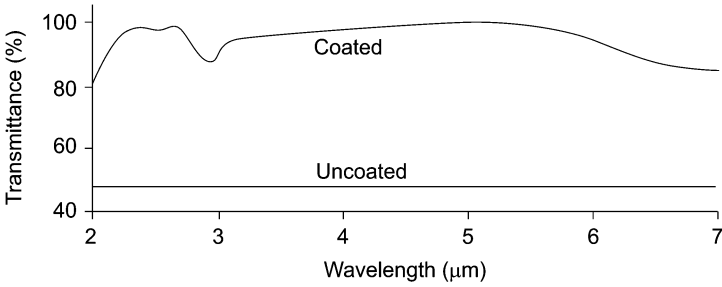


**Figure 3.14.** Measured transmittance of a germanium plate with coatings consisting of  $\text{MgF}_2 + \text{CeO}_2 + \text{Si}$  ( $n_1 d_1 = n_2 d_2 = n_3 d_3 = \lambda/4$  at  $3.5 \mu\text{m}$ ). (After Cox *et al* [5].)

eliminate those which are not. Performance can then be accurately calculated by the procedures of chapter 2.

A particularly useful technique of this type has been developed by Musset and Thelen [6]. It is based on Smith’s method, that is, the method of effective interfaces. We recall from chapter 2 that this involves the breaking down of the assembly into two subsystems. These we can label a and b. The overall transmittance of the multilayer is then given by

$$T = \left[ \frac{T_a T_b}{\left(1 - R_a^{1/2} R_b^{1/2}\right)^2} \right] \times \left[ 1 + \frac{4R_a^{1/2} R_b^{1/2}}{\left(1 - R_a^{1/2} R_b^{1/2}\right)^2} \sin^2 \left( \frac{\varphi_a + \varphi_b - 2\delta}{2} \right) \right]^{-1} \quad (3.13)$$

We assume that there is no absorption, so that  $T_a = 1 - R_a$  and  $T_b = 1 - R_b$ .

Both of the expressions multiplied together on the right-hand side of equation (3.13) have maximum possible values of unity, and for maximum transmittance, therefore, both must be separately maximised. The first expression

$$\frac{T_a T_b}{\left(1 - R_a^{1/2} R_b^{1/2}\right)^2}$$

will be unity if, and only if,  $R_a = R_b$ , while the second,

$$\left[ 1 + \frac{4R_a^{1/2} R_b^{1/2}}{\left(1 - R_a^{1/2} R_b^{1/2}\right)^2} \sin^2 \left( \frac{\varphi_a + \varphi_b - 2\delta}{2} \right) \right]^{-1}$$

will be unity if, and only if,

$$\sin^2 \left( \frac{\varphi_a + \varphi_b - 2\delta}{2} \right) = 0.$$

The conditions for a perfect antireflection coating are then

$$R_a = R_b$$

called the amplitude condition by Musset and Thelen, and

$$\frac{\varphi_a + \varphi_b - 2\delta}{2} = m\pi$$

called the phase condition. The amplitude condition is a function of the two subsystems. The phase condition can be satisfied by adjusting the thickness of the spacer layer. The amplitude condition can, using a method devised by Musset and Thelen, be satisfied for all wavelengths, but it is difficult to satisfy the phase condition except at a limited number of discrete wavelengths. At other wavelengths the performance departs from ideal to a varying degree.

The transmittance and reflectance of a multilayer remain constant when the optical admittances are all multiplied by a constant factor or when they are all replaced by their reciprocals, in both cases keeping the optical thicknesses constant. These properties can readily be demonstrated from the structure of the characteristic matrices [7]. They enable the design of pairs of substructures having identical reflectance so that only the phase condition need be satisfied for perfect antireflection. We can, following Musset and Thelen, imagine a multilayer consisting of two subsections, a and b, as shown in figure 3.15, with a medium of admittance  $y_i$  in between. At this stage we put no restrictions on this medium in terms either of refractive index or thickness but, as we shall see, they will become defined at a later stage. Subsection a is bounded by  $y_m$  on one side and  $y_i$  on the other, while b is bounded in the same way by  $y_i$  and  $y_0$ . We can now apply the appropriate rules for ensuring that the amplitude condition is satisfied. We set up any subsystem a and then convert it into subsystem b by retaining the optical thicknesses and either multiplying the admittances by a constant multiplier, or taking the reciprocals of the admittances and multiplying them by a constant multiplier. Systems derived by the former procedure are classified by Musset and Thelen as type I, those by the latter as type II.

For type I systems we must have

$$\begin{aligned} y_m f &= y_i \\ y_i f &= y_0 \end{aligned}$$

so that

$$y_i = (y_0 y_m)^{1/2}$$

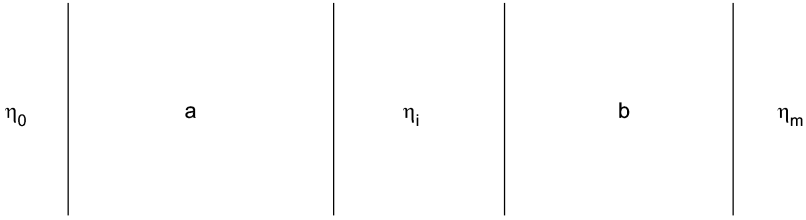


**Figure 3.15.** Multilayer antireflection coating consisting of two subsystems, a and b, separated by a central layer.

and

$$f = (y_0/y_m)^{1/2}.$$

In this way, any  $y_a$  gives a corresponding  $y_b$  of  $y_a(y_0/y_m)^{1/2}$ .

Type II systems, on the other hand, convert so that

$$\begin{aligned} f/y_m &= y_0 \\ f/y_i &= y_i \\ f/y_a &= y_b, \end{aligned}$$

i.e.

$$y_i = (y_0 y_m)^{1/2} \quad \text{and} \quad f = y_0 y_m$$

so that any  $y_a$  gives a corresponding  $y_b$  of  $y_0 y_m / y_a$ .

There are no restrictions on layer thickness or on the number of layers in each subsystem except that they must be equal in number, and it is simpler if quarter-wave layers are used. Once the individual subsystems a and b are established, the amplitude condition is automatically satisfied at all wavelengths and it remains to satisfy the phase condition. This involves the coupling arrangement. It is impossible to meet the phase condition at all wavelengths and the problem is so complex that it is best to take the easy way out and adopt a layer of admittance  $y_i$  with thickness zero, in which case the layer is omitted, or a quarter-wave, like the remaining layers of the assembly.

The method can be illustrated by application to the antireflection of germanium at normal incidence. In this case,  $n_0 = 1.00$  and  $n_m = 4.00$ . Hence  $n_i = (n_0 n_m)^{1/2} = 2.0$  in both type I and II systems. First of all we take, for subsystem a, a straightforward single quarter-wave matching the substrate to the coupling medium:

$$n_1 \left| \begin{array}{c} n_a \\ (n_i n_m)^{1/2} \end{array} \right| n_m \\ 2.0 \left| \begin{array}{c} 2.826 \\ 4.0. \end{array} \right|$$

## Chapter 4

---

# Neutral mirrors and beam splitters

### 4.1 High-reflectance mirror coatings

Almost as important as the transmitting optical components of the previous chapter are those whose function is to reflect a major portion of the incident light. In the vast majority of cases the sole requirement is that the specular reflectance should be as high as conveniently possible, although, as we shall see, there are specialised applications where not only should the reflectance be high, but also the absorption should be extremely low. For mirrors in optical instruments, simple metallic layers usually give adequate performance and these will be examined first. For some applications where the reflectance must be higher than can be achieved with simple metallic layers, their reflectance can be boosted by the addition of extra dielectric layers. Multilayer all-dielectric reflectors, which combine maximum reflectance with minimum absorption, and which transmit the energy which they do not reflect, are reserved for the next chapter.

#### 4.1.1 Metallic layers

The performance of the commonest metals used as reflecting coatings is shown [1] in figure 4.1.

Aluminium is easy to evaporate and has good ultraviolet, visible and infrared reflectance, together with the additional advantage of adhering strongly to most substances, including plastics. As a result it is the most frequently used film material for the production of reflecting coatings. The reflectance of an aluminium coating does drop gradually in use, although the thin oxide layer, which always forms on the surface very quickly after coating, helps to protect it from further corrosion. In use, especially if the mirror is at all exposed, dust and dirt invariably collect on the surface and cause a fall in reflectance. The performance of most instruments is not seriously affected by a slight drop in reflectance, but in some cases where it is important to collect the maximum amount of light, as it is difficult to clean the coatings without damaging them, the components

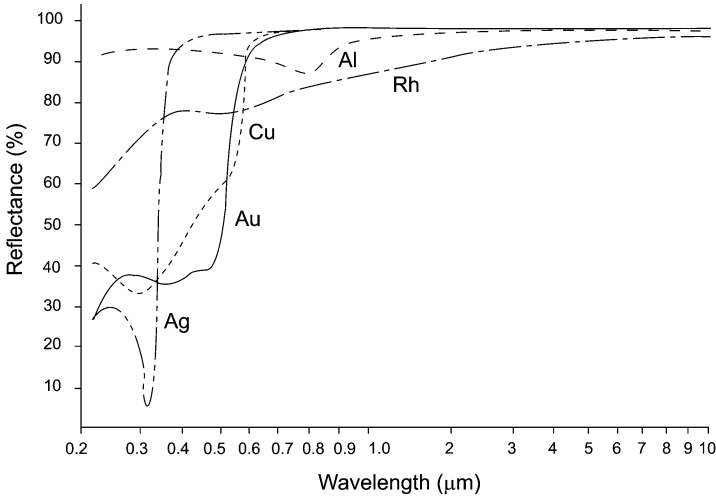


**Figure 4.1.** Reflectance of freshly deposited films of aluminium, copper, gold, rhodium and silver as a function of wavelength from 0.2–10  $\mu\text{m}$  (After Hass [1].)

are recoated periodically. This applies particularly to the mirrors of large astronomical reflecting telescopes. The primary mirrors of these are recoated with aluminium usually around once a year in coating plants which are installed in the observatories for this purpose. Because the primaries are very large and heavy (for example, the 98-inch primary of the Isaac Newton Memorial Telescope of the Royal Greenwich Observatory weighs some 9000 lb), it is not usual to rotate them during coating and the uniformity of coating is achieved through the use of multiple sources.

Silver was once the most popular material of all. It does tarnish when exposed to the atmosphere, owing mainly to the formation of silver sulphide, but the initial high reflectance and the extreme ease of evaporation still make it a common choice for components used only for a short period of time. Silver is also often used where it is necessary to coat temporarily a component, such as an interferometer plate, for a test of flatness.

Gold is probably the best material for infrared reflecting coatings. Its reflectance drops off rapidly in the visible region and it is really useful only beyond 700 nm. On glass, gold tends to form rather soft, easily damaged films, but it adheres strongly to a film of chromium or Nichrome, and this is often used as an underlayer between the gold and the glass substrate.

The reflectance of rhodium and platinum is much less than that of the other metals mentioned and these metals are used only where stable films very resistant to corrosion are required. Both materials adhere very strongly to glass.

### 4.1.2 Protection of metal films

Most metal films are rather softer than hard dielectric films and can be scratched easily. Unprotected evaporated aluminium layers, for example, can be badly damaged if wiped with a cloth, while gold and silver films are even softer. This is a serious disadvantage, especially when periodic cleaning of the mirrors is necessary. One solution, as we have seen, is periodic recoating. An alternative, which improves the ruggedness of the coatings and also protects them from atmospheric corrosion, is overcoating with an additional dielectric layer. The behaviour of a single dielectric layer on a metal is a useful illustration of the calculation techniques of chapter 2. We shall also require some related results later and so it is useful to spend a little time on the problem.

First of all, the admittance diagram (figure 4.2) gives us a qualitative picture of the behaviour of the system as the dielectric layer is added. The metal layer will normally be thick enough for the optical admittance at its front surface to be simply that of the metal, the substrate optical constants having no effect. The optical admittance of the metal will always be in the fourth quadrant and so, as a dielectric layer is added, the reflectance must fall until the locus of the admittance of the assembly crosses the real axis. (The reflectance associated with the locus of a dielectric layer of index higher than the incident medium always falls as the locus is traced out in the fourth quadrant and always rises in the first—figure 2.11(a).) This minimum of reflectance will occur at a dielectric layer thickness of less than a quarter-wave. For layer thicknesses of up to twice this figure, therefore, the reflectance of the protected metal film will be reduced. The reduction in reflectance depends very much on the particular metal and the index of the dielectric film.

We can mark the position of the quarter-wave dielectric layer thickness by a simple construction. We draw the line from the origin to the starting point of the dielectric locus, that is the metal admittance  $(\alpha, -\beta)$  which lies in the fourth quadrant. This line makes an angle  $\theta$  with the real axis. Then, also through the origin, we draw a line in the first quadrant making the same angle  $\theta$  with the real axis. This cuts the dielectric locus in two points. One is the point  $(\alpha, \beta)$ , the image of the starting point in the real axis, and at this point the reflectance of the assembly is identical to that of the uncoated metal. The second point of intersection is

$$\left( \frac{\eta_f^2 \alpha}{(\alpha^2 + \beta^2)}, \frac{\eta_f^2 \beta}{(\alpha^2 + \beta^2)} \right) \quad \text{i.e.} \quad \frac{\eta_f^2}{\alpha - i\beta}$$

and at this point the layer is one quarter-wave thick.

We can derive straightforward analytical expressions for the various parameters, and, in particular, the points of intersection of the locus with the real axis, which we know correspond to the points of maximum and minimum reflectance.

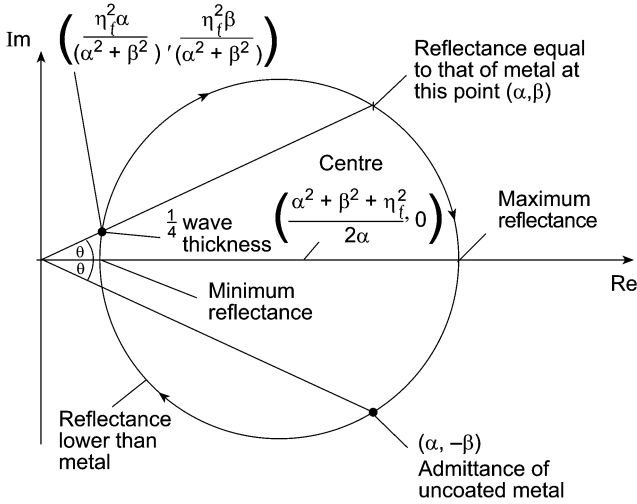


**Figure 4.2.** Admittance diagram of a dielectric layer deposited over a metal. The metal admittance would usually be much closer to the imaginary axis but has been moved for greater clarity in the diagram. The dielectric locus starts at the admittance of the uncoated metal. The construction to find the quarter-wave point is explained in the text, as are the other parameters.

The characteristic matrix is given by

$$\begin{bmatrix} B \\ C \end{bmatrix} = \begin{bmatrix} \cos \delta_f & i(\sin \delta_f / \eta_f) \\ i\eta_f \sin \delta_f & \cos \delta_f \end{bmatrix} \begin{bmatrix} \alpha - i & 1 \\ \beta & \beta \end{bmatrix} \quad (4.1)$$

where  $\alpha - i\beta$  is the characteristic admittance of the metal, i.e.  $\mathcal{Y}(n_m - ik_m)$  at normal incidence,  $\delta_f = 2\pi n_f d_f \cos \theta_f / \lambda$ , and  $\eta_f$  is the characteristic admittance of the film material. Then

$$\begin{bmatrix} B \\ C \end{bmatrix} = \begin{bmatrix} \cos \delta_f + (\beta \sin \delta_f) / \eta_f + i(\alpha \sin \delta_f) / \eta_f \\ \alpha \cos \delta_f + i(\eta_f \sin \delta_f - \beta \cos \delta_f) \end{bmatrix}.$$

Now, at the points of intersection of the locus with the real axis, we must have that the admittance, which we can denote by  $\mu$ , is real. But

$$\mu = C / B$$

and, equating real and imaginary parts,

$$\alpha \cos \delta_f = \mu [\cos \delta_f + (\beta \sin \delta_f) / \eta_f] \quad (4.2)$$

$$\eta_f \sin \delta_f - \beta \cos \delta_f = \mu (\alpha \sin \delta_f) / \eta_f. \quad (4.3)$$

Hence, first eliminating  $\mu$ ,

$$(\alpha \cos \delta_f)(\alpha \sin \delta_f) / \eta_f = (\eta_f \sin \delta_f - \beta \cos \delta_f) [\cos \delta_f + (\beta \sin \delta_f) / \eta_f]$$

i.e.

$$[(\alpha^2 + \beta^2 - \eta_f^2)/(2\eta_f)] \sin(2\delta_f) = -\beta \cos(2\delta_f).$$

Thus

$$\tan(2\delta_f) = 2\beta\eta_f/(\eta_f^2 - \alpha^2 - \beta^2)$$

so that

$$\delta_f = \frac{1}{2} \tan^{-1}[2\beta\eta_f/(\eta_f^2 - \alpha^2 - \beta^2)] + \frac{m\pi}{2} \quad m = 0, 1, 2, 3 \dots \quad (4.4)$$

or, in full waves,

$$D_f/\lambda_0 = (1/4\pi) \tan^{-1}[2\beta\eta_f/(\eta_f^2 - \alpha^2 - \beta^2)] + m/4 \quad (4.5)$$

where the arctangent is to be taken in either the first or second quadrant so that  $\delta_f$  for  $m = 0$  is positive and represents the first intersection with the real axis where the film is less than, or at the very most, equal to a quarter-wave. A similar result has been derived by Park [2] using a slightly different technique.

The value of  $\mu$  can be found by rearranging equations (4.2) and (4.3) slightly:

$$\begin{aligned} (\mu - \alpha) \cos \delta_f + (\beta\mu/\eta_f) \sin \delta_f &= 0 \\ \beta \cos \delta_f + [(\mu\alpha/\eta_f) - \eta_f] \sin \delta_f &= 0 \end{aligned}$$

and, eliminating  $\delta_f$ ,

$$(\mu - \alpha)[(\mu\alpha/\eta_f) - \eta_f] - \beta(\beta\mu/\eta_f) = 0.$$

The two solutions are

$$\mu = [(\alpha^2 + \beta^2 + \eta_f^2)/2\alpha] \pm \{[(\alpha^2 + \beta^2 + \eta_f^2)/4\alpha^2] - \eta_f^2\}^{1/2}$$

but this is not the best form for calculation. We know that the two solutions  $\mu_1$  and  $\mu_2$  are related by  $\mu_1\mu_2 = \eta_f^2$  and so we write

$$\mu_1 = 2\alpha\eta_f^2/\{(\alpha^2 + \beta^2 + \eta_f^2) + [(\alpha^2 + \beta^2 + \eta_f^2)^2 - 4\alpha^2\eta_f^2]^{1/2}\} \quad (4.6)$$

$$\mu_2 = [(\alpha^2 + \beta^2 + \eta_f^2)/2\alpha] + \{[(\alpha^2 + \beta^2 + \eta_f^2)/4\alpha^2] - \eta_f^2\}^{1/2} \quad (4.7)$$

and the value which corresponds to the first intersection ( $m = 0$  in equation (4.4)) is

$$\mu_1 = 2\alpha\eta_f^2/\{(\alpha^2 + \beta^2 + \eta_f^2) + [(\alpha^2 + \beta^2 + \eta_f^2)^2 - 4\alpha^2\eta_f^2]^{1/2}\}. \quad (4.6)$$

Often

$$(\alpha^2 + \beta^2 + \eta_f^2)^2 \gg 4\alpha^2\eta_f^2$$

Table 4.1.

Aluminium (0.82 – i5.99)	$R_{\text{uncoated}}$ (%)	$R_{\text{min}}$ (%)	$D_{\text{min}}$ (Full waves)	$R_{\text{max}}$ (%)	$D_{\text{max}}$ (Full waves)
Quartz (1.45)	91.63	83.64	0.2128	91.86	0.4628
CeO <sub>2</sub> (2.30)	91.63	65.90	0.1925	92.44	0.4425

and in that case

$$\mu_1 = \alpha \eta_f^2 / (\alpha^2 + \beta^2 + \eta_f^2) \quad (4.8)$$

$$\mu_2 = (\alpha^2 + \beta^2 + \eta_f^2) / \alpha. \quad (4.9)$$

The limits of reflectance are given by

$$R_{\text{minimum}} = [(\eta_0 - \mu_1) / (\eta_0 + \mu_1)]^2 \quad (4.10)$$

$$R_{\text{maximum}} = [(\eta_0 - \mu_2) / (\eta_0 + \mu_2)]^2. \quad (4.11)$$

The higher the index of the dielectric film, the greater is the fall in reflectance at the minimum. The reflectance rises above that of the bare metal at the maximum, but, for the metals commonly used as reflectors, the increase is not great, and so the lower-index films are to be preferred as protecting layers. As an example, we can consider aluminium, which has a refractive index of 0.82 – i5.99 at 546 nm [3], with protecting layers of quartz of index 1.45 or a high-index layer, 2.3, such as cerium oxide. The results in table 4.1 were calculated from equations (4.5)–(4.7), (4.10) and (4.11). Clearly, if high-index films are used for protecting metal layers, then the monitoring of layer thickness must be accurate, otherwise there is a risk of a sharp drop in reflectance.

Aluminium is probably the commonest mirror coating material for the visible region, and, in addition to the quartz and cerium oxide mentioned above, there is a large number of materials which can be used for protecting it. Silicon oxide, SiO<sub>2</sub>, for example, is also a very effective protecting material, but it has strong absorption at the blue end of the spectrum, where it causes the reflectance of the composite coating to be rather low. Another useful coating is sapphire Al<sub>2</sub>O<sub>3</sub>. This can be vacuum deposited, or the aluminium at the surface of the coating can be anodised by an electrolytic technique [1], forming a very hard layer of aluminium oxide. Gold and silver are more difficult to protect because of the difficulty of getting films to stick to them. However, it has been found that aluminium oxide sticks very well to silver [4,5]. Aluminium oxide does not appear to be a very effective barrier against moisture and so it has been used principally as a bonding layer between the silver and a layer of silicon oxide which affords good moisture resistance and which, although it adheres only weakly to silver, adheres strongly to the aluminium oxide. Further details of the coating are

given by Hass and his colleagues [4]. To reduce the absorption at the blue end of the spectrum, the silicon oxide should be reactively deposited (see chapter 9) when the actual oxide which is produced lies between  $\text{SiO}$  and  $\text{SiO}_2$ . With such a coating it is possible to achieve a reflectance greater than 95% over the visible and infrared from 0.45–20  $\mu\text{m}$ .

Aluminium oxide and silicon oxide are absorbing at wavelengths longer than 8  $\mu\text{m}$  and it has been discovered by Pellicori [6] and confirmed theoretically by Cox *et al* [5] that reflectors protected by these materials exhibit a sharp dip in reflectance at high angles of incidence, that is, 45° and above. The dip can be avoided by the use of a protecting material which does not absorb in this region. Magnesium fluoride is such a material, but it must be deposited on a hot substrate (temperatures in excess of 200 °C) if it is to be robust. The metals have their best performance if deposited at room temperature and thus the substrates should only be heated after they have been coated with the metal.

#### 4.1.3 Overall system performance, boosted reflectance

In optical instruments of any degree of complexity there will be a number of reflecting components in series, and the overall transmission of the system will be given by the product of the reflectances of the various elements. Figure 4.3 gives the overall transmission of any system with a number of components in series, with identical values of reflectance. It is obvious from the diagram that even with the best metal coatings, the performance with ten elements, say, is low. If the instrument is to be used over a wide range there is little that can be done to alleviate the situation. Most spectrometers, for instance, have ten or more reflections with a consequent severe drop in transmission, but are required to work over a wide region—possibly as much as a 25:1 variation in wavelength. The spectrometer designer normally just accepts this loss and designs the rest of the instrument accordingly.

In cases where the wavelength range is rather more limited, say, to the visible region or to a single wavelength, it is possible to increase the reflectance of a simple metal layer by boosting it with extra dielectric layers.

The characteristic admittance of a metal can be written  $n - ik$  and the reflectance in air at normal incidence is

$$R = \left| \frac{1 - (n - ik)}{1 + (n - ik)} \right|^2 = \frac{(1 - n)^2 + k^2}{(1 + n)^2 + k^2} = \frac{1 - [2n/(1 + n^2 + k^2)]}{1 + [2n/(1 + n^2 + k^2)]}. \quad (4.12)$$

On p 53 it was shown that the optical admittance of an assembly  $Y$  becomes  $n^2/Y$  when a quarter-wave optical thickness of index  $n$ , that is admittance in free space units, is added.

If the metal is overcoated with two quarter-waves of material of indices  $n_1$  and  $n_2$ ,  $n_2$  being next to the metal, then the optical admittance at normal incidence

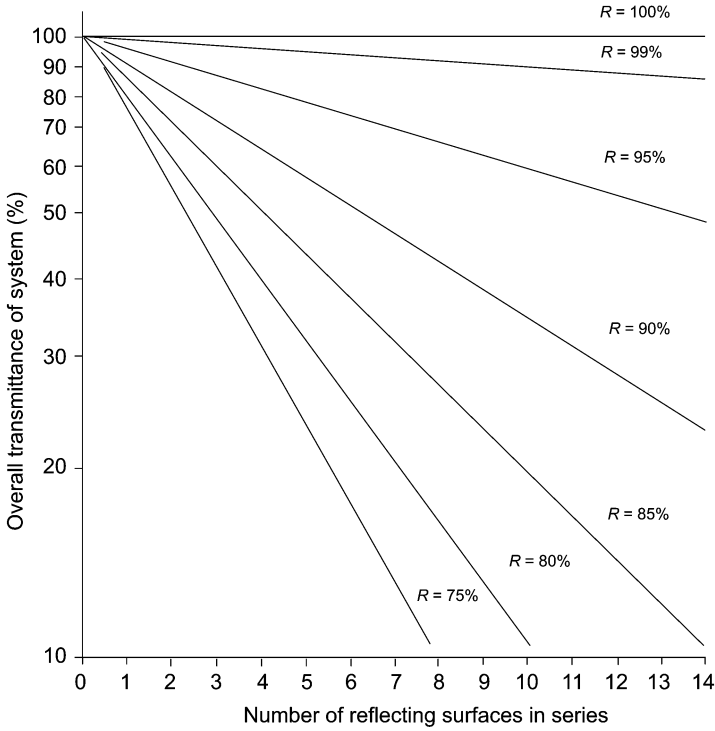


**Figure 4.3.** Overall transmittance of an optical system which has a number of reflecting elements in series.

is

$$\left(\frac{n_1}{n_2}\right)^2 (n - ik)$$

and the reflectance in air, also at normal incidence,

$$R = \left| \frac{1 - (n_1/n_2)^2(n - ik)}{1 + (n_1/n_2)^2(n - ik)} \right|^2$$

i.e.

$$\begin{aligned} R &= \frac{[1 - (n_1/n_2)^2n]^2 + (n_1/n_2)^4k^2}{[1 + (n_1/n_2)^2n]^2 + (n_1/n_2)^4k^2} \\ &= \frac{1 - [2(n_1/n_2)^2n]/[1 + (n_1/n_2)^4(n^2 + k^2)]}{1 + [2(n_1/n_2)^2n]/[1 + (n_1/n_2)^4(n^2 + k^2)]}. \end{aligned} \tag{4.13}$$

This will be greater than the reflectance of the bare metal, given by

equation (4.12), if

$$\frac{2(n_1/n_2)^2 n}{1 + (n_1/n_2)^4 (n^2 + k^2)} < \frac{2n}{1 + n^2 + k^2} \quad (4.14)$$

which is satisfied by either

$$\left(\frac{n_1}{n_2}\right)^2 > 1$$

or

$$\left(\frac{n_1}{n_2}\right)^2 < \frac{1}{n^2 + k^2} \quad (4.15)$$

assuming that  $n^2 + k^2 \geq 1$ .

The first solution is of greater practical value than the second, which can be ignored. This shows that the reflectance of any metal can be boosted by a pair of quarter-wave layers for which  $(n_1/n_2) > 1$ ,  $n_1$  being on the outside and  $n_2$  next to the metal. The higher this ratio, the greater the increase in reflectance. As an example, consider aluminium at 550 nm with  $n - ik = 0.92 - i5.99$ . From equation (4.12), the untreated reflectance of this is approximately 91.6%.

If the aluminium is covered by two quarter-waves consisting of magnesium fluoride of index 1.38, next to the aluminium, followed by zinc sulphide of index 2.35, then  $(n_1/n_2)^2 = 2.9$  and, from equation (4.13), the reflectance jumps to 96.9%.

An approximate result can be obtained very quickly using  $A = (1 - R)$ . When the two layers are added,  $A$  is reduced roughly to  $A/(n_1/n_2)^2$ . Inserting the above figures, for aluminium,  $A$  is 8.4% initially, and on addition of the layers drops to 2.9%, corresponding to a boosted reflectance of 97.1% (instead of the more accurate figure of 96.9%).

A second similar pair of dielectric layers will boost the reflectance even higher—to approximately 99%, and greater numbers of quarter-wave pairs may be used to give an even higher reflectance.

Unfortunately, the region over which the reflectance is boosted is limited. Outside this zone the reflectance is less than it would be for the bare metal. Jenkins [7] has measured the reflectance of an aluminium layer overcoated with six quarter-wave layers of cryolite, of index 1.35, and zinc sulphide of index 2.35. With layers monitored at 550 nm, the reflectance of the boosted aluminium was greater than 95% over a region 280 nm wide, and greater than 99% over the major part.

More robust coatings can be obtained using magnesium fluoride, silicon dioxide or aluminium oxide as the low-index layers, and cerium oxide or titanium oxide as the high-index layers. To attain maximum toughness, the dielectric layers should be deposited on a hot substrate. Aluminium, however, if deposited hot, tends to scatter badly and so the substrates should be heated only after deposition

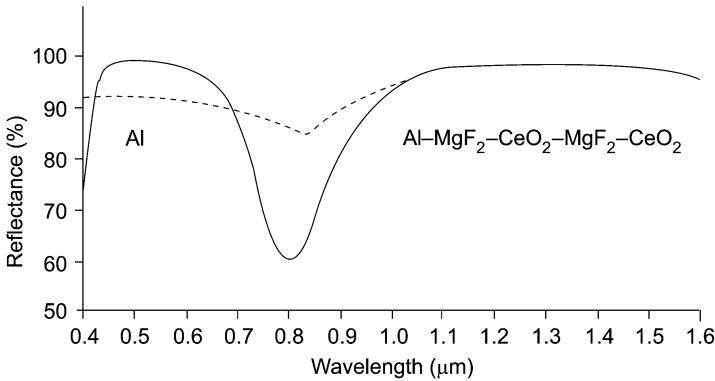


**Figure 4.4.** Reflectance of evaporated aluminium with (solid curve) and without (dashed curve) two reflectance-increasing film pairs of  $\text{MgF}_2$  and  $\text{CeO}_2$  as a function of wavelength from 0.4–1.6  $\mu\text{m}$ . (After Hass [1].)

of the aluminium is complete. Figure 4.4 shows the reflectance of aluminium boosted by four quarter-wave layers, which enhanced the reflectance over the visible region.

We have already considered more exactly the behaviour of a single dielectric layer on a metal, and have shown, as did Park [2], that the thickness of the dielectric layer for minimum reflectance should be

$$D = \{\tan^{-1}[2\beta\eta_f/(\eta_f^2 - \alpha^2 - \beta^2)]\}[\lambda_0/(4\pi)]$$

where  $(\alpha - i\beta)$  is the admittance of the metal and the angle is in the first or second quadrant. This is the thickness which the low-index layer next to the metal should have if the maximum possible increase in reflectance is to be achieved. A moment's consideration of the admittance diagram will show that this is indeed the case. Layers other than that next to the metal will, of course, retain their quarter-wave thicknesses.

#### 4.1.4 Reflecting coatings for the ultraviolet

The production of high-reflectance coatings for the ultraviolet is a much more exacting task than for the visible and infrared. A very full review of the topic is given by Madden [8], supplemented in great detail by a later account by Hass and Hunter [9]. The following is a very brief summary.

The most suitable material known for the production of reflecting coatings for the ultraviolet out to around 100 nm is aluminium. To achieve the best results, the aluminium should be evaporated at a very high rate, 40 nm s<sup>-1</sup> or more if possible, on to a cold substrate, the temperature of which should not be permitted to exceed 50 °C, and at pressures of 10<sup>-6</sup> torr or lower. The aluminium should be

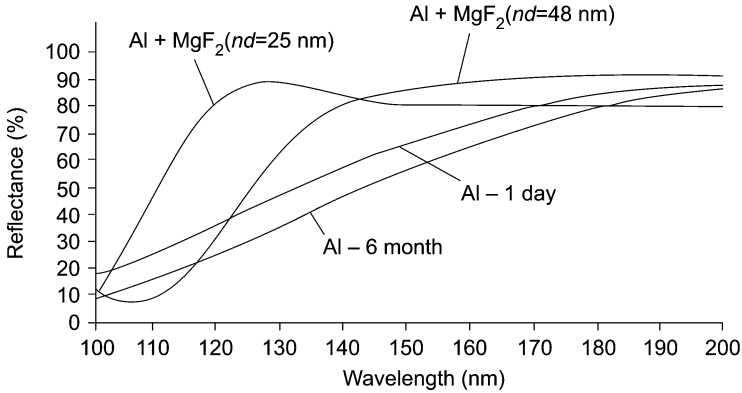


**Figure 4.5.** Reflectance of evaporated aluminium from 100–200 nm with and without protective layers of MgF<sub>2</sub> of two different thicknesses. (After Canfield *et al* [11].)

of the purest grade. Hass and Tousey [10] have quoted results which show that there is a significant improvement (as high as 10% at 150 nm) in the ultraviolet reflectance of aluminium films if 99.99% pure aluminium is used in preference to 99.5% pure. Aluminium should, in theory, have a much higher reflectance than is usually achieved in practice, particularly at the shortwave end of the range. This has been found to be due to the formation of a thin oxide layer on the surface, and as we have already shown, such a layer must, unless it is very thick, lead to a reduction in reflectance. This oxidation takes place even at partial pressures of oxygen below  $10^{-6}$  torr. Unprotected aluminium films, therefore, inevitably show a rapid fall in reflectance with time when exposed to the atmosphere. The reflectance stabilises when the layer is of sufficient thickness to inhibit further oxidation, but this occurs only when the reflectance at short wavelengths has fallen catastrophically.

Attempts have been made to find suitable protecting material for aluminium to prevent oxidation, and very promising results have been obtained with magnesium fluoride (very robust coatings) and lithium fluoride (less robust), which in crystal form are very useful window materials for the ultraviolet. Figures 4.5 and 4.6 show the effect of an extra protecting layer of magnesium fluoride [11] or lithium fluoride [12] on the reflectance of aluminium. The increase in reflectance is partly due to the lack of oxide layer, but also to interference effects.

It is necessary to evaporate the protecting layer immediately after the aluminium in order that the minimum amount of oxidation should be allowed to take place. This is usually achieved by running the two sources simultaneously and arranging for the shutter which covers the aluminium source at the end of the deposition of the aluminium layer to uncover at the same time the magnesium or lithium fluoride source. The use of magnesium fluoride overcoated aluminium as

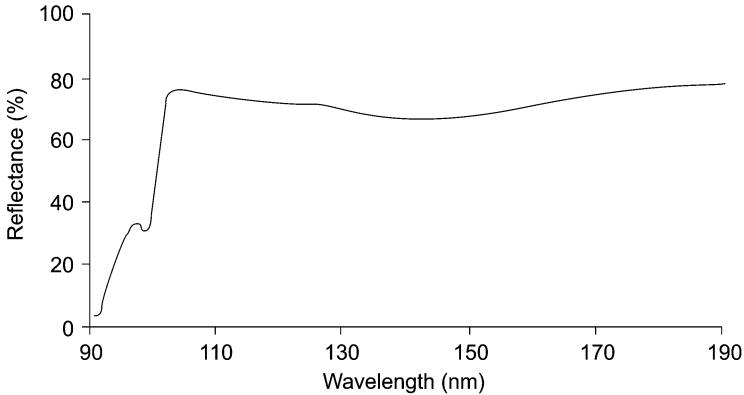


**Figure 4.6.** Reflectance of an evaporated aluminium film with a 14-nm thick LiF overcoating in the region of 90–190 nm. Measurements were begun 10 minutes after the evaporation was completed. (After Cox *et al* [12].)

a reflecting coating for the ultraviolet is now becoming standard practice.

The aluminium and magnesium fluoride coating is examined in some detail by Canfield *et al* [11]. Amongst other results they show that provided the magnesium fluoride is thicker than 10 nm the coatings will withstand, without deterioration, exposure to ultraviolet radiation and to electrons (up to  $10^{16}$ , 1 MeV electrons/cm<sup>2</sup>) and protons (up to  $10^{12}$ , 5 MeV protons/cm<sup>2</sup>).

## 4.2 Neutral beam splitters

A device which divides a beam of light into two parts is known as a beam splitter. The functional part of a beam splitter generally consists of a plane surface coated to have a specified reflectance and transmittance over a certain wavelength range. The incident light is split into a transmitted and a reflected portion at the surface, which is usually tilted so that the incident and reflected beams are separated. The ideal values of reflectance and transmittance may vary from one application to another. The beam splitters considered in this section are known as neutral beam splitters, because reflectance and transmittance should ideally be constant over the wavelength range concerned.

Neutral beam splitters are usually specified by the ideal values of transmittance and reflectance expressed as a percentage and written  $T/R$ . 50/50 beam splitters are probably the most common.

### 4.2.1 Beam splitters using metallic layers

Apart from a single uncoated surface, which is sometimes used, the simplest type of beam splitter consists of a metal layer deposited on a glass plate. Silver,

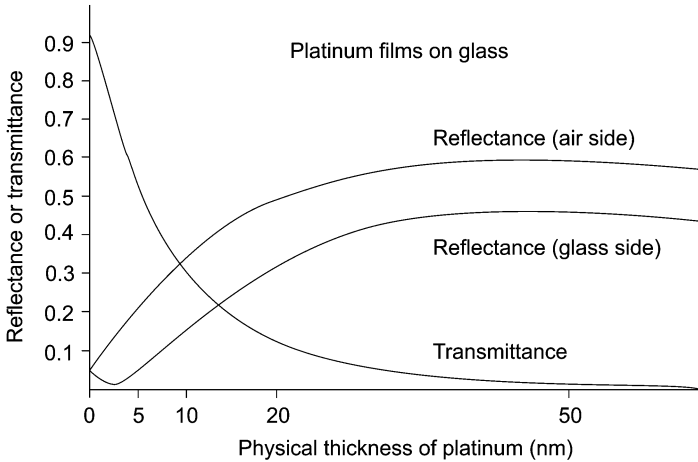


**Figure 4.7.** Reflectance and transmittance curves for a platinum film on glass, calculated from the optical constants on the bulk metal. (After Heavens [13].)

which has least absorption of all the common metals used in the visible region, is traditionally the most popular material for this. 50/50 beam splitters are frequently referred to as being ‘half-silvered’, although commercial beam splitters nowadays are usually constructed from metals such as chromium which are less prone to damage by abrasion and corrosion.

All metallic beam splitters suffer from absorption. The transmission of a metal film is the same, regardless of the direction in which it is measured. This is not so for reflectance, and that measured at the air side is slightly higher than that measured at the glass side. This effect does not appear with a transparent film. Since  $T + A + R = 1$ , the reduction in reflectance at the substrate side means that the absorption from that side must always be higher. Figure 4.7 shows curves for platinum demonstrating this behaviour [13]. Because of this difference in reflection, metallic beam splitters should always be used in the manner shown in figure 4.8 if the highest efficiency is to be achieved.

It is possible to decrease the absorption in metallic beam splitters by adding an extra dielectric layer. The method has been applied to chromium films by Pohlack [14] and figure 4.9 gives some of the measurements made.

The first pair of results is for a simple chromium film on glass of index 1.52 measured both from the air side and the glass side. The second pair of results shows how the absorption in the chromium can be reduced by the presence of a quarter-wave layer of high refractive index material (zinc sulphide of index approximately 2.4 in this case) between the metal and the glass. This layer forms an antireflection coating on the rear surface of the metal, and the effect can be seen particularly strongly in the results for reflectance and transmission from the glass side. There, the transmission remains exactly as before, but the reflectance